Scaling Effects of Turbulence-induced Forcing Function in the Core Support Barrel due to Impingement Flow from a Cold-leg Piping

Sang Gyu Lim[a*], Byong Jo Yun[b], Jae Min Lee[a], Sun Hee Choi[a], Kyu Hyung Kim[a], Do Young Ko[a], Do Hwan Lee[a]
[a]*KHNP Central Research Institute, 1312 70-gil Yuseong-daero, Yuseong-gu, Deajeon, 34101, Korea*
[b]*Pusan National University, Mechanical Engineering Dept., 2, Busandaehak-ro 63beon-gil, Geumjeong-gu, Busan, 46241, Korea*
[*]*Corresponding author: sanggyu.lim@khnp.co.kr*

1. Introduction

Nuclear Power Plants (NPPs) had experienced flow, acoustic, and mechanical-induced vibrations during their service life. The regulatory body required a comprehensive vibration assessment program (CVAP) to an applicant or licensee to demonstrate that there were no adverse vibration or excessive loading for the reactor internals. The CVAP for prototype reactor internals, a first-of-a-kind or unique design, includes a vibration and stress analysis, vibration measurement, inspection, and correlation of predicted and measured results to demonstrate the acceptable performance of reactor internals in the normal steady-state and anticipated transient operation of the nuclear power plant [1].

Before determining the design loads, a methodology for hydraulic forcing functions should be validated based on a validated scale model test (SMT) and/or data acquired from other plants. Korea Hydro and Nuclear Power Company Ltd. (KHNP) will perform an SMT for APR1400 reactor internals. For designing of an SMT facility, scaling ratios and relevant non-dimensional numbers should be carefully selected to conserve the flow-induced vibration phenomena of the prototype.

This paper investigated scaling effects of turbulence-induced forcing function in the core support barrel (CSB) in the SMT when the cold-leg flow impinged to the CSB during normal operation. First, an ideal scaling law and a similarity criterion were derived from reference papers. Next, computational fluid dynamics (CFD) analysis was performed to compare the hydraulic forcing functions on the CSB in three cases, a prototype, a reduced velocity condition in the SMT, a conserved velocity condition in the SMT.

2. Scaling Law and Similarity Criterion

2.1 Scaling Law

Over a few decades, many researchers have been suggested scaling laws for thermal-hydraulic experiments [3,4,5,6]. Each of the scaling laws has its advantages and disadvantages. A linear scaling law is that the length of the model is linearly scaled down as a geometric scale ratio $\frac{l_m}{l_p} = \lambda$ and time scale τ between the prototype and the model is equal to the geometric scale λ. For the linear scaling law, the fluid velocity of the model must be kept equal to the prototype. But the acceleration scale between the model and the prototype is equal to $1/\lambda$. Therefore, the linear scaling law is suitable for an inertia force-dominant system, but it is not suitable for a gravitational force-dominant system such as natural circulation phenomena.

In the SMT, the turbulence-induced forcing function is dominated by the inertia force of pump operation. Therefore, we selected the linear scaling law. Major scaling ratios for the linear scaling law were presented in Table I.

Table I: Major Scaling Ratios

Parameter	Linear scaling ratio
Length	λ
Area	λ^2
Velocity	1
Gravity	$1/\lambda$
Time	$\tau = \lambda$

2.2 Similarity Criterion

Au-Yang [7] carried out the SMT to obtain the turbulence-induced forcing functions on the CSB. The turbulence-induced forcing functions were compared with field test data of Babcock and Wilcox pressurized water reactor (PWR). To compare the forcing function between the SMT and the field test, he adopted the non-dimensional parameter, called the normalized power spectral densities (PSD).

$$\phi = \frac{\mathrm{G(f)}}{\rho^2 U^4 (\frac{\delta}{U})} = \frac{\mathrm{G(f)}}{\rho^2 U^3 \delta} \quad (1)$$

where, $\mathrm{G(f)}$ is the pressure PSD in (pressure)^2/Hz, ρ is the fluid density, U is a characteristic velocity, the downcommer mean velocity is used in this case, δ is a characteristic length, a gap width of the downcomer is chosen in this case.

The frequency of the forcing function in each of the model and prototype is not the same. To compare the normalized PSD between the model and the prototype, the frequency of the forcing function should be non-dimensionalized. Thus, Au-Yang suggested the reduced frequency.

$$F = \mathrm{f}\frac{\delta}{\mathrm{U}} \quad (2)$$

where, f is the turbulence-induced pressure fluctuation frequency in Hz.

If $\phi_p = 1$ and $F_p = 1$ in the prototype, the model should satisfied $\phi_m = 1$ and $F_m = 1$. Here, the subscript p is the prototype, the subscript m is the model.

For the similarity criterion of the normalized PSD,

$$\frac{\phi_m}{\phi_p} = \frac{G_m}{G_p}\left(\frac{\rho_m}{\rho_p}\right)^{-2}\left(\frac{U_m}{U_p}\right)^{-3}\left(\frac{\delta_m}{\delta_p}\right)^{-1} = 1 \quad (3)$$

where, $\frac{\rho_m}{\rho_p} \cong 1$, $\frac{U_m}{U_p} = 1$ (Linear scaling law), $\frac{\delta_m}{\delta_p} = \lambda$.

Therefore, the similarity criterion is,

$$\frac{G_m}{G_p} = \lambda \quad \rightarrow G_m = \lambda G_p \quad (4)$$

For the similarity criterion of the reduced frequency,

$$\frac{F_m}{F_p} = \frac{f_m}{f_p}\frac{\delta_m}{\delta_p}\left(\frac{U_m}{U_p}\right)^{-1} = 1 \quad (5)$$

where, $\frac{U_m}{U_p} = 1$ (Linear scaling law), $\frac{\delta_m}{\delta_p} = \lambda$.

Therefore, the similarity criterion is,

$$\frac{f_m}{f_p} = \frac{1}{\lambda} \quad \rightarrow f_m = \frac{1}{\lambda} f_p \quad (6)$$

Au-Yang selected the geometrical scale ratio $\lambda = 1/6$, but the velocity scale ratio is $\frac{U_m}{U_p} = \frac{1}{2}$ *or* $\frac{1}{3}$. Strictly speaking, he violated the ideal scaling ratio of the linear scaling law.

Meanwhile, the normalized PSD of the model was qualitatively similar to the normalized PSD of the field test data but quantitatively not identical. In summary, Au-Yang showed that the turbulence-induced forcing function of the prototype could be conserved in the SMT from the viewpoint of the engineering approach even though the velocity scale ratio $\frac{U_m}{U_p}$ is not the same as unity.

Although his pioneering research results, the violation of the velocity scaling ratio in the linear scaling law is still questionable.

To verify this problem, KHNP will maintain the velocity scaling ratio $\frac{U_m}{U_p} = 1$ in the SMT, and Reynolds number dependency test will be conducted with varying the flow velocity up to the prototype velocity.

3. CFD Analysis for Scaling Effects

3.1 Analysis Models and Boundary Conditions

The objectives of this analysis is to check a tendency and an inter-relationship of the normalized PSD between the models and the prototype. Also, this analysis can give us insights into the CFD validation items for the turbulence-induced forcing functions. ANSYS CFX version 19.2 was used for this analysis.

As shown in Fig. 1, a quarter of the full downcomer for apr14000 was modeled to reduce the numerical cost. To simplify the problem, the hot-leg nozzle in the downcomer and lower support structures and internals of the reactor were removed in the analysis model. We focused on the hydraulic forcing function on the CSB.

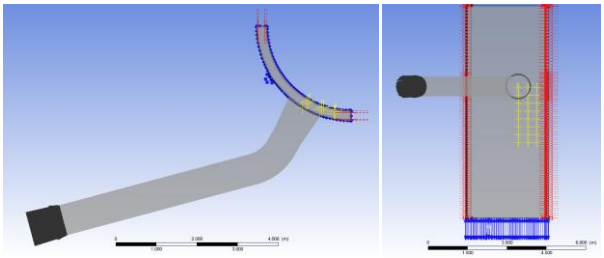

Fig. 1. CFD geometrical model (left: top view, right: side view).

Major analysis models and boundary conditions were summarized in Table II.

Table II: Major analysis models and boundary conditions

Analysis models	Details		
Geometrical models	Prototype	1/5 model (SMT)	1/5 model (SMT)
Velocity Scale ratio	1	1/2 (Reduced Velocity)	1 (Conserved Velocity)
Turbulence model	Detached Eddy Simulation (Initialized by SST model)		
Time step	5.0e-5 sec		
Mesh type/ number of mesh	Hexagonal mesh/ Total number of elements = 21Million		
Min. first layer thickness	0.03mm/Growth rate=1.2		

Note that analysis models and mesh systems were not fully validated. The CFD analysis methodology will be validated using the SMT results.

3.2 Analysis results and discussions

Fig. 2 showed the streamlines in the downcomer for each model. The streamline distribution was similar to each other, but the streamline of the secondary flow after impingement on the CSB wall was slightly different from each other at the below of the cold-leg position.

Fig. 3 illustrated the local mean velocity distribution along with the axial height of the downcomer. The similar distribution of three cases was shown in Fig. 3.

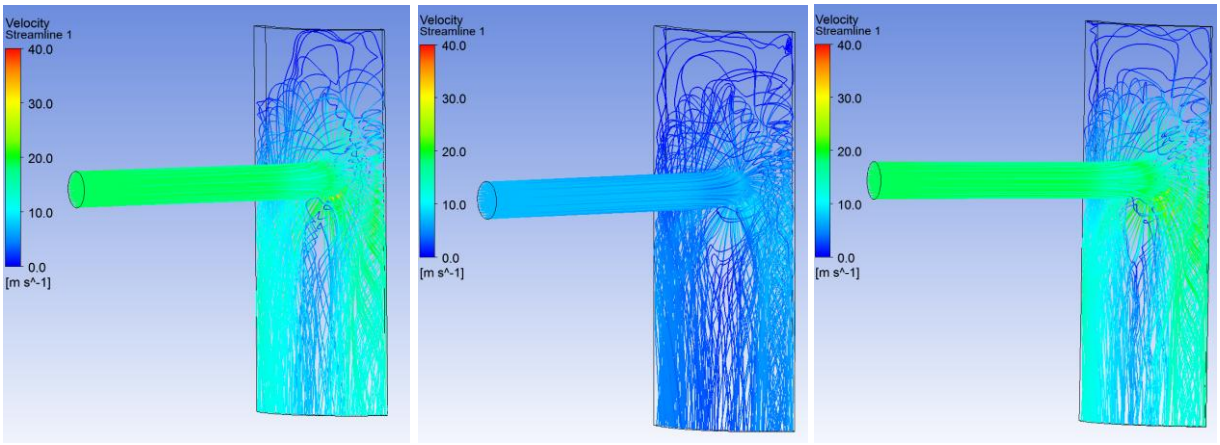

Fig. 2. Streamline for each model (left: prototype, middle: SMT-reduced velocity, right: SMT-conserved velocity).

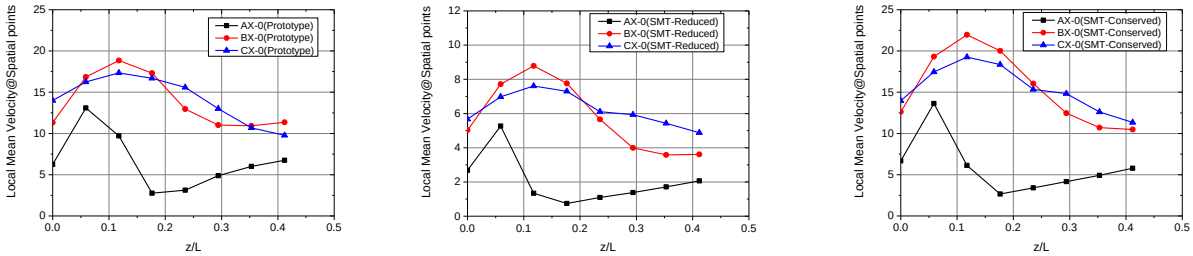

Fig. 3. Local mean velocity distribution along the axial height of the downcomer (left: prototype, middle: SMT-reduced velocity, right: SMT-conserved velocity).

In accordance with Au-Yang's methodology, the normalized PSD of three cases can be compared in the reduced frequency domain. To obtain the local dynamic pressure fluctuation in the downcomer, a total of 72 of the monitoring points were generated during the transient analysis, as illustrated in Fig. 4.

Among the analysis results, the maximum pressure PSDs were observed at the A6-2 location in three cases. The maximum pressure PSDs were presented in Fig. 5 with the upper bound correlation of Au-Yang's experiment [8]. The upper bound forcing function correlations in Au-Yang's experiment are,

$$\phi = 0.155e^{-3.0F} \quad 0 < \mathrm{F} < 1.0 \tag{7}$$

$$\phi = 0.027e^{-1.26F} \quad 1.0 < \mathrm{F} < 5.0 \tag{8}$$

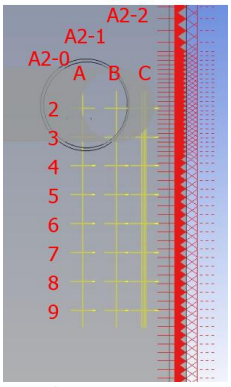

Fig. 4. Monitoring points for the local dynamic pressure fluctuation in the CFD model.

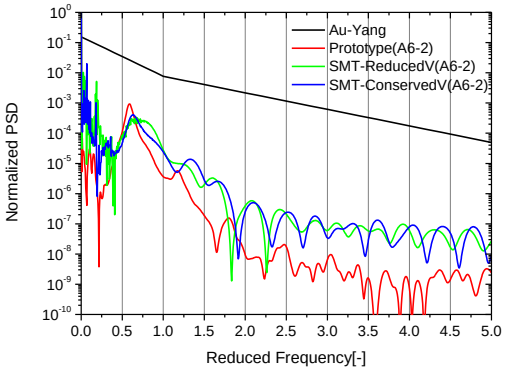

Fig. 5. The calculated maximum normalized PSD in the reduced frequency domain.

As shown in Fig. 5, the calculated maximum pressure PSDs were similar to the three cases, and the calculated results were less than the upper bound of the Au-Yang correlation.

To satisfy the similarity between the model and prototype in the linear scaling law, Eq. (4) and Eq. (6) should be met. Assuming that the Au-Yang's normalized PSD is still well working even though the velocity scaling ratio is 1/2, Eq. (4) and Eq. (6) are changed to Eq. (9) and Eq. (10). Here, the geometrical scaling ratio $\lambda = 1/5$.

$$\frac{G_m}{G_p} = \frac{\lambda}{2^3} \rightarrow G_m = \frac{\lambda}{8} G_p = 0.025 G_p \tag{9}$$

$$\frac{f_m}{f_p} = \frac{1}{2\lambda} \rightarrow f_m = \frac{1}{2\lambda} f_p = 2.5 f_p \tag{10}$$

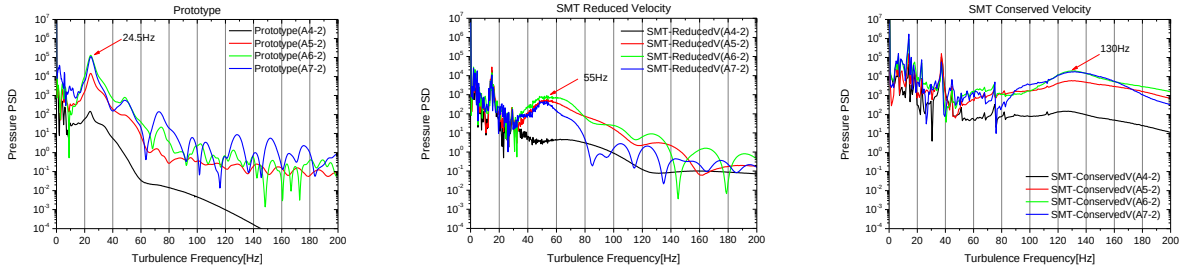

Fig. 6. Pressure PSD versus turbulence frequency (left: prototype, middle: SMT-reduced velocity, right: SMT-conserved velocity).

Table III: Comparison of the calculated turbulence frequency and the pressure PSD based on the ideal linear scaling law

Variables	Turbulence frequency			Pressure PSD		
Cases	Prototype	1/5 model (Reduced Velocity)	1/5 model (Conserved Velocity)	Prototype	1/5 model (Reduced Velocity)	1/5 model (Conserved Velocity)
Ideal scaling law	f_p	$f_m = 2.5 f_p$	$f_m = 5 f_p$	G_p	$G_m = 0.025 G_p$	$G_m = 0.2 G_p$
Expected ideal variables	$f_p = 24.5Hz$	$f_m = 61.25Hz$	$f_m = 122.5Hz$	$G_p = 128{,}790$	$G_m = 3{,}220$	$G_m = 25{,}758$
Calculated variables	$24.5Hz$	$55Hz$	$130Hz$	128,790 $(Pa)^2/Hz$	730 $(Pa)^2/Hz$	19,850 $(Pa)^2/Hz$
Difference $(\frac{Calculated-Expected}{Expected})$	-	-10.2%	+6.1%	-	-77.3%	-22.9%

Fig. 6 presented the pressure PSD in the frequency domain of turbulence pressure fluctuation. In the prototype results, we can pick the turbulence frequency at the maximum pressure PSD point, as highlighted in Fig. 6. The calculated turbulence frequency of the prototype is about 24.5 Hz.

Based on Au-Yang's methodology, the ideal turbulence frequency of the scale model should be increased. As described in Table III, the ideal turbulence frequency of the models can be calculated. The differences between the expected ideal frequency and the calculated frequency are within ±10%, which means that the Au-Yang's methodology is well working even in the reduced velocity condition in the SMT case.

Meanwhile, the difference of the pressure PSDs between the prototype and the two SMT cases became much larger than the turbulence frequency. Notably, the pressure PSD in the reduced velocity condition of the SMT was predicted about -77.3% of the ideal pressure PSD. By the way, the calculated pressure PSD in the conserved velocity condition of the SMT approached to the ideal value rather than the reduced velocity condition.

Lee [3] noticed that flow-induced vibration is weak dependent on Reynolds number according to a scaling analysis. In summary, the reduced velocity condition may not ideally conserve the turbulence fluctuation amplitude even though the turbulence fluctuation frequency of the reduced velocity condition is well conserved in the SMT. Note that this CFD analysis is a preliminary calculation for checking the tendency of the scaling effects so that we will investigate the Reynolds number dependency and the similarity of the turbulence fluctuation amplitude with varying the flow velocity in the SMT.

3. Conclusions

The ideal scaling laws for the pressure PSD and the reduced frequency were derived based on the linear scaling law and Au-Yang's methodology. For two design options of the SMT scale, 1/5 scale of SMT with the reduced velocity and 1/5 scale of SMT with the conserved velocity were suggested to check the tendency of the scaling effects.

The turbulence frequencies in both the reduced velocity and the conserved velocity were well predicted within ±10% of the difference between the calculated frequency and the ideal frequency. In contrast, the turbulence fluctuation amplitude in the reduced velocity may not be conserved rather than the conserved velocity. Therefore, we will maintain the velocity scaling ratio is unity. Also, the similarity of the turbulence frequency and amplitude will be validated in the scale model test and the CFD analysis.

REFERENCES

[1] Nuclear Regulatory Commission, Regulatory Guide 1.20(Rev.4) Comprehensive Vibration Assessment Program for Reactor Internals During Preoperational and Startup Testing, U.S. NRC, Feb. 2017.

[2] H. Lee, Fluid-Elastic Parameters for Reactor Internals Model Testing, Journal of the Korean Nuclear Society, Vol.12, pp.286-292, 1980.

[3] R. L. Kiang, Scaling Criteria for Nuclear Reactor Thermal Hydraulics, Nuclear Science and Engineering, Vol.89, pp. 207-216, 1985.
[4] A. M. Nahavandi, F. S. Castellana, E. N. Moradkhanian, Scaling Laws for Modeling Nuclear Reactor Systems, Nuclear Science and Engineering, Vol.72, pp. 75-83, 1979.
[5] M. Ishii, Scaling Laws for Thermal-Hydraulic System under Single Phase and Two-phase Natural Circulation, Nuclear Engineering and Design, Vol.81, pp. 411-425, 1984.
[6] B.J. Yun, H.K. Cho, D.J. Euh, C.H. Song, G.C. Park, Scaling for the ECC Bypass Phenomena During the LBLOCA Reflood Phase, Nuclear Engineering and Design, Vol. 231, pp. 315-325, 2004.
[7] M.K. Au-Yang, Dynamic Pressure Inside a PWR – A Study Based on Laboratory and Field Test Data, Nuclear Engineering and Design, Vol. 58, pp. 113-125, 1980.
[8] M.K. Au-Yang, Flow-induced Vibration of Power and Process Plant Components: A Practical Workbook, ASME Press, New York, pp. 235, 2001.